Mechanism and significance of chlorophyll breakdown

Christ, Bastien ; Hörtensteiner, Stefan

Abstract: Chlorophyll breakdown is the most obvious sign of leaf senescence and fruit ripening. A multistep pathway has been elucidated in recent years that can be divided into two major parts. In the first phase, which commonly is active in higher plants, chlorophyll is converted via several photoreactive intermediates to a primary colorless breakdown product within the chloroplast. The second part of chlorophyll breakdown takes place in the cytosol and the vacuole. During this phase, the primary colorless intermediate is modified in largely species-specific reactions to a number of similar, yet structurally different, linear tetrapyrrolic products that finally are stored within the vacuole of senescing cells. To date, most of the biochemical reactions of the first phase of chlorophyll breakdown have been elucidated and genes have been identified. By contrast, mechanisms of catabolite transport and modification during the second phase are largely unknown. This review summarizes the current knowledge on the biochemical reactions involved in chlorophyll breakdown, with a special focus on the second-phase reactions and the fate of by-products that are released from chlorophyll during its breakdown.

DOI: https://doi.org/10.1007/s00344-013-9392-y

Mechanism and Significance of Chlorophyll Breakdown

Bastien Christ[1] and Stefan Hörtensteiner[2]

Institute of Plant Biology, University of Zurich, CH-8008 Zurich, Switzerland

[1]bastien.christ@botinst.uzh.ch

[2]Corresponding author, phone: +41 44 634 82 82, fax: +41 44 634 82 04, shorten@botinst.uzh.ch

ABSTRACT

Chlorophyll breakdown is the most obvious sign of leaf senescence and fruit ripening. A multi-step pathway has been elucidated in recent years that can be divided into two major parts. In the first phase that is commonly active in higher plants chlorophyll is converted via several photoreactive intermediates to a primary colorless breakdown product within the chloroplast. The second part of chlorophyll breakdown takes place in the cytosol and the vacuole. During this phase, the primary colorless intermediate is modified in largely species-specific reactions to a number of similar, yet structurally different, linear tetrapyrrolic products that finally are stored within the vacuole of senescing cells. To date, most of the biochemical reactions of the first phase of chlorophyll breakdown have been elucidated and genes been identified. By contrast, mechanisms of catabolite transport and modification during the second phase are largely unknown. This review summarizes the current knowledge on the biochemical reactions involved in chlorophyll breakdown with a special focus on the phase two reactions and the fate of by-products that are released from chlorophyll during its breakdown.

KEY WORDS

chlorophyll breakdown, chlorophyll catabolites, detoxification, nutrient remobilization, senescence

A. INTRODUCTION

Chlorophyll (Chl) breakdown is the hallmark of senescence because of its impact on the color of senescing organs: loss of green Chls unmasks yellow carotenoids and highlights the synthesis of red anthocyans. Why do plants degrade Chls? Chloroplasts have been shown to contain up to 75% of the nitrogen content in photosynthetic tissues (Peoples and Dalling 1988; Makino and Osmond 1991). Rubisco, the most abundant protein of the chloroplast, accounts for 20–30% of total leaf nitrogen and protein complexes of the thylakoids such as photosystems (PS) constitute the second largest pool of chloroplast nitrogen (Hörtensteiner and Feller 2002; Feller et al. 2008). During senescence and remobilization of chloroplast nutrients, Chls are uncoupled from Chl-binding proteins within the PS and become phototoxic. Therefore, coordinated Chl breakdown maintains cell viability during senescence and allows an efficient remobilization of nutrients to growing organs.

Most enzymes involved in Chl degradation are now characterized and form the so-called "PAO pathway" (Fig. 1). This pathway can be divided into two main parts. The first one occurs within the chloroplast at the thylakoid membrane and involves phototoxic catabolites. The second part of the PAO pathway consists of modifications of colorless Chl catabolites and their translocation from the chloroplast to the vacuole. Recently, new insights have been obtained on the topology of Chl degradation within the chloroplast as well as on cytosolic modifications of colorless catabolites. The aim of this review is to provide an updated summary of the PAO pathway and to discuss its biological functions.

B. THE PAO PATHWAY

B.1 Detoxification of colored chlorophyll catabolites in the chloroplast

B.1.1 Conversion of Chl *b* to *a*

Chl *b* is converted to Chl *a* by the action of two enzymes, Chl *b* REDUCTASE (CBR) and 7-HYDROXYMETHYL Chl *a* REDUCTASE (HCAR; Fig. 1; Tanaka and Tanaka 2011). Plants possess two isoforms of CBR called NON-YELLOW COLORING1 (NYC1) and NYC1-LIKE (NOL; Kusaba et al. 2007; Sato et al. 2009). *In silico* hydrophobicity analysis of NYC1 and NOL protein sequences predicted NYC1 to be a

membrane protein and NOL to be a soluble protein (Kusaba et al. 2007). Furthermore, *in vitro* immunoprecipitation and localization experiments in rice (*Oryza sativa*) suggested that the two proteins could form heterodimers at the thylakoid membrane (Kusaba et al. 2007; Sato et al. 2009). Although only NOL activity has been demonstrated *in vitro*, the two enzymes are thought to catalyze the same reaction, i. e. the reduction of Chl *b* to 7-hydroxymethyl Chl *a* (HMChl *a*). Interestingly, an *Arabidopsis* (*Arabidopsis thaliana*) *nyc1 nol* double mutant does not show an altered Chl *a*/*b* ratio during the unstressed vegetative phase, but displays a stay-green phenotype during leaf senescence and seed maturation due to the retention of Chl *b* (Horie et al. 2009). Taken together, these data suggest that NYC1 and NOL do not participate actively to Chl *a*/*b* ratio regulation during the vegetative growth, but are required for developmental processes such as leaf senescence (Tanaka and Tanaka 2011). Finally, Chl *b* to *a* reduction appears to be crucial for light harvesting complex (LHC) degradation during senescence since *nyc1 nol* mutants retain particularly LHC proteins (Kusaba et al. 2007; Horie et al. 2009).

Recently, the enzyme catalyzing the second step of Chl *b* to Chl *a* reduction, conversion of HMChl *a* to Chl *a*, was characterized in *Arabidopsis* (Meguro et al. 2011). HCAR contains a flavin adenine dinucleotide and an iron-sulfur center as cofactors, and phylogenetic analysis revealed that HCAR evolved from divinyl chlorophyllide reductase of the Chl biosynthesis pathway (Meguro et al. 2011). HCAR is able to catalyze the conversion of HMChl *a* to Chl *a* *in vitro* and T-DNA insertion mutants for HCAR accumulate low levels of HMChl *a* during leaf senescence. Surprisingly, *hcar* mutants retain significant amounts of pheophorbide (Pheide) *a*, a downstream intermediate of the Chl degradation pathway. Pheide *a* OXYGENASE (PAO, the enzyme catalyzing the degradation of Pheide; see below) protein levels were unchanged in *hcar* as compared to wild-type plants. These observations, together with the fact that Pheide *a* accumulates in a *hcar nyc1 nol* triple mutant, suggest that HMChl or some degradation products of HMChl could inhibit PAO activity by an unknown mechanism, resulting in the accumulation of Pheide *a* (Meguro et al. 2011).

There are strong evidences that the first step of Chl *b* degradation is its conversion to Chl *a*. The main argument is that PAO is specific for the "*a*" form of Pheide (Hörtensteiner et al. 1995; Pružinská et al. 2003). In addition, *nyc1 nol* mutants are unable to degrade Chl *b* during leaf senescence. As mentioned above, *nyc1 nol* mutants retain large amounts of LHC protein indicating that Chl *b* to *a* conversion is a prerequisite for both LHC and Chl *b* degradation. Finally, it has been shown that Chl *b* to *a* conversion must precede demetalation and

dephytylation because HCAR is able to reduce HMChl *a in vitro* but not 7-hydroxymethyl pheophytin *a* or 7-hydroxymethyl Pheide *a* (Shimoda et al. 2012). All together, these data indicate that Chl *b* to *a* conversion is necessary for Chl *b* and Chl *b*-containing complex, i.e. LHC, degradation, and that Chl *b* to *a* conversion (but not demetalation or dephytylation) is the first step of Chl *b* degradation. Thus, Chl *a* degradation seems to be independent of Chl *b* to *a* reduction. In line with this, *Arabidopsis nyc1 nol* degrades Chl *a* and PS core complexes as wild-type (Horie et al. 2009). Furthermore, *nyc1 cao* double mutants of rice, in which the entire Chl cycle (interconverting Chl *a* and Chl *b*) is abolished, solely produce Chl *a* during vegetative growth and are able to degrade it during leaf senescence (Kusaba et al. 2007).

Interestingly, it has been demonstrated that overproduction of Chl *b* in *Arabidopsis* leads to the incorporation of Chl *b* into PS core complexes, which seems to partially inhibit their degradation during senescence (Hirashima et al. 2006; Sakuraba et al. 2010; Shimoda et al. 2012; Sakuraba et al. 2012a). These findings indicate that Chl *b* to *a* conversion has evolved specifically to act on LHC complexes. It is interesting to note that Chl *b* overproduction in *Arabidopsis* appears to also retard age-dependent senescence via transcriptional down-regulation of senescence associated genes (SAG; Sakuraba et al. 2012a). Incorporation of Chl *b* in PS core complexes, and their consequent increased stability, is thought to maintain active PS during the senescence phase. The increased photosynthetic capacity resulting from Chl *b* overproduction could modulate *SAG* expression through an unknown signaling pathway (Sakuraba et al. 2012a).

B.1.2 Destabilization of Chl-apoprotein complexes by STAY-GREEN

Deletion of the chloroplast-localized protein STAY-GREEN (SGR), as the name implies, causes a stay-green phenotype (Hörtensteiner 2009). Conversely, many but not all mutations triggering a stay-green phenotype affect the *SGR* gene. Among more than 14 stay-green mutants identified in natural populations, mutagenesis screens or breeding programs of different plant species, eight are deficient of SGR (Hörtensteiner 2009; Schelbert et al. 2009). Notably, presence or absence of a functional *SGR* gene in pea (*Pisum sativum*) determines the color of the cotyledons (green or yellow), originally described by Mendel (Mendel 1866; Armstead et al. 2007). Furthermore, the commercial tomato (*Solanum lycopersicum*) variety "*green-flesh"* is also deficient in SGR (Barry et al. 2008). The brown coloration of ripe *green-flesh* fruits is due to Chl retention and simultaneous carotenoid accumulation.

The exact role of the SGR protein, which does not contain any known domain, is still unclear (Hörtensteiner 2009). Suppression of *SGR* leads to a cosmetic stay-green phenotype (Jiang et al. 2007; Park et al. 2007; Ren et al. 2007), i.e. photosynthesis capacity of *sgr* mutants during leaf senescence decreases as in corresponding wild-types. However, several LHC and core subunits of PSI and II are partially retained (Jiang et al. 2007; Park et al. 2007; Aubry et al. 2008). Together with the finding that SGR can interact with LHC proteins of PSII (Park et al. 2007), these observations suggest that SGR participates in the destabilization of Chl-apoprotein complexes of PSII during senescence. Recently, this hypothesis has been corroborated by the finding that SGR plays a central role in recruiting Chl catabolic enzymes (CCE) at the thylakoid membrane (Sakuraba et al. 2012b; Sakuraba et al. 2013).

Interestingly, SGR seems to also have other functions, not directly related to Chl degradation. SGR appears to be implicated in root nodule senescence (Zhou et al. 2011). Root nodules of legume species such as *Medicago sativa* and *Medicago truncatula* are specialized organs hosting soil bacteria capable of reducing atmospheric nitrogen to ammonium. Nodule senescence stops nitrogen fixation and results in the loss of the symbiotic interaction. Silencing of *SGR* in *M. truncatula* was shown to affect nodule senescence, and thus indicates that SGR could also have a function in non-photosynthetic tissues (Zhou et al. 2011). Recently, SGR has been shown to regulate lycopene and β-carotene biosynthesis in tomato fruits (Luo et al. 2013). SGR directly interacts with PHYTOENE SYNTHASE 1, a carotenoid synthetic enzyme and thereby inhibits its activity. These two studies clearly demonstrate that SGR, besides its requirement for Chl breakdown, is also involved in other biochemical processes.

B.1.3 Demetalation

With regard to the recent knowledge acquired about dephytylation of Chl during leaf senescence (see below), it is likely that demetalation precedes dephytylation and thus occurs on Chl *a* (Fig. 1; Morita et al. 2009; Schelbert et al. 2009; Ren et al. 2010; Shimoda et al. 2012). To date, the mechanism involved in Chl demetalation is unknown (Hörtensteiner 2012). Several biochemical approaches described the involvement of either a heat-stable metal-chelating substance (MCS) or a metal-releasing protein (MRP; Vicentini et al. 1995; Shioi et al. 1996a; Suzuki and Shioi 2002; Büchert et al. 2011). All these studies used chlorophyllin (an artificial and soluble

147 Chl derivative) as substrate, but not Chl (Hörtensteiner 2012). A recent proteomic study of plastoglobules in
148 *Arabidopsis* annotated a possible MRP protein (Lundquist et al. 2012). However, analysis of T-DNA insertion
149 lines in this gene did not show any delay in Chl degradation during dark-induced senescence (Luzia Guyer and
150 Stefan Hörtensteiner, unpublished data). Release of Mg^{2+} from Chl is known to occur at slightly acidic pH (Saga
151 and Tamiaki 2012). Thus, it can be speculated that the decrease of photosynthesis during senescence lowers the
152 stromal pH sufficiently to remove Mg^{2+} from the Chl macrocycle. Thereby, SGR could have a decisive role;
153 during vegetative growth, the stromal pH also decreases at night, but absence of senescence-regulated SGR,
154 which is thought to destabilize Chl-apoprotein complexes (Park et al. 2007), could avoid massive demetalation
155 of Chls before the onset of senescence.
156
157 B.1.4 Dephytylation
158
159 Already one century ago, Willstätter and Stoll described an enzyme, called CHLOROPHYLLASE (CLH), that
160 was able to cleave the phytol tail of Chls (Willstätter and Stoll 1911) thereby producing chlorophyllide. Later,
161 Mayer et al. (1930) found CLH activity in several plant species and Holden (1961) partially purified CLHs from
162 sugar beet (*Beta vulgaris*) and pea and further characterized their activity (Mayer 1930; Holden 1961). To date,
163 more than 250 studies have been performed on plant CLHs according to the Web of Knowledge database (search
164 performed with "chlorophyllase(s)" in titles). The majority of these studies describe the (partial) purification of
165 CLHs from different plant species and the characterization of their *in vitro* activity. Cloning of CLH genes from
166 plants such as *Chenopodium album*, *Arabidopsis* and citrus (*Citrus sinensis*) revealed that CLHs contain a lipase
167 motif. In addition, gene transcription of most CLHs is highly induced by ethylene and JA treatments, which are
168 known to promote senescence (Jakob-Wilk et al. 1999; Tsuchiya et al. 1999). However, two CLHs (*Arabidopsis*
169 *At*CLH2 and *C. album Ca*CLH) are not induced by phytohormones and show constitutively low levels of
170 expression (Jakob-Wilk et al. 1999; Tsuchiya et al. 1999). Using biochemical and immunolocalization
171 approaches, several studies could localize CLH to the chloroplast (Brandis et al. 1996; Matile et al. 1997;
172 Harpaz-Saad et al. 2007; Azoulay-Shemer et al. 2011). In citrus, CLH appears to be post-translationally
173 regulated by N- and C-terminal proteolysis within chloroplast membranes and mature CLH was shown to be
174 more active than the CLH precursor (Harpaz-Saad et al. 2007; Azoulay-Shemer et al. 2011). Collectively
175 considered, all these data suggest a major role for CLH in hydrolyzing the phytol chain of Chl. However, reverse
176 genetic approaches of CLH-deficient plants did not corroborate this hypothesis (Benedetti and Arruda 2002;

177 Schenk et al. 2007). Although silencing of *Arabidopsis At*CLH1 (*Arabidopsis* has two CLH homologues) was
178 believed to decrease chlorophyllide/Chl ratios in green leaves, analysis of T-DNA insertion mutant lines for
179 *At*CLH1 (*clh1*) and *At*CLH2 (*clh2*) did not reveal any delay of Chl degradation during senescence in single as
180 well as in double mutants (Benedetti and Arruda 2002; Schenk et al. 2007). Decrease and increase of
181 chlorophyllide/Chl ratios caused by, respectively, silencing and overexpressing of CLH in *Arabidopsis* reported
182 by Bendetti et al. (2002) could be experimental artefacts and may reflect the *in vitro* rather than the *in vivo*
183 activity of CLH. Indeed, in this study, extraction of green pigments from plant tissue was performed in acetone
184 at 4°C during 12 h. However, CLH has been reported to be active *in vitro* under such conditions (Barrett and
185 Jeffrey 1964). Lastly, the hypothesis that *Arabidopsis* CLHs are not involved in Chl degradation during age-
186 dependent and dark-induced leaf senescence is corroborated by the finding that *At*CLHs are located in the
187 cytosol of senescent cells (Schenk et al. 2007).
188
189 The question how the phytol group of Chl may be hydrolyzed during age-dependent leaf senescence remained
190 unanswered until recently. Using an elegant *in silico* approach in *Arabidopsis*, Schelbert et al. (2009) could
191 identify a chloroplast-targeted serine-type hydrolase, the mutation of which leads to a stay-green phenotype
192 during leaf senescence (Schelbert et al. 2009). Surprisingly, this senescence-induced hydrolase is not active on
193 Chl *in vitro* but was found to specifically hydrolyze the phytol chain of pheophytin (Phein) and to produce
194 Pheide. The protein, termed Phein Pheide HYDROLASE (PPH), was shown to be indispensable for Chl
195 degradation during leaf senescence in *Arabidopsis* and rice (Morita et al. 2009; Schelbert et al. 2009; Ren et al.
196 2010). *Arabidopsis pph* mutants are also affected in LHC and PS core subunit degradation, indicating that phytol
197 cleavage, in addition to Chl *b* to *a* reduction (see above), is crucial for degradation of PS proteins during leaf
198 senescence (Schelbert et al. 2009).
199
200 B.1.5 Opening and reduction of the macrocycle
201
202 The light absorption capacity of tetrapyrroles and thus the potential phototoxicity of some Chl catabolites is
203 mostly due to electron conjugation within the porphyrin ring (Hörtensteiner 2006; Scheer 2006; Hörtensteiner
204 and Kräutler 2011). Opening of the macrocycle of Pheide *a* by PAO and the subsequent reduction of the
205 conjugated C20/C1 double bond of the intermediate, red Chl catabolite (RCC), by RCC REDUCTASE (RCCR)
206 are the two steps of the Chl degradation pathway that lead to the loss of Chl catabolite phototoxicity (Fig. 1;

Hörtensteiner 2006; Hörtensteiner and Kräutler 2011). Thus, *primary* fluorescent Chl catabolite (*p*FCC), the product of the consecutive PAO and RCCR activities, is considered as non-phototoxic (Hörtensteiner 2006; Hörtensteiner and Kräutler 2011; Hörtensteiner 2012).

The enzymatic activities responsible for opening of the Pheide macrocycle and production of *p*FCC were originally detected in isolated intact gerontoplasts and were shown to be promoted by the supply of glucose-6-phosphate or ATP (Schellenberg et al. 1990; Matile et al. 1992). Later, *p*FCC production from Pheide was shown to be possible *in vitro* by using isolated thylakoid membranes and reduced ferredoxin (Schellenberg et al. 1993; Ginsburg et al. 1994). Partial purification of this activity from *Brassica napus* revealed its dependency on a stromal fraction, senescence inducibility and specificity towards Pheide *a*, i. e. Pheide *b* not being a substrate (Hörtensteiner et al. 1995). Dependency of the activity on a stromal fraction was explained by the finding that the conversion of Pheide to *p*FCC was a two-step reaction performed by two enzymes, one localized in chloroplast membranes (PAO) and the other in the stroma (RCCR; Rodoni et al. 1997). For a long time, PAO was considered to localize to the chloroplast envelope but recent reconsideration of Chl catabolic enzyme localization revealed that PAO is rather inserted into the thylakoid membrane (Matile et al. 1996; Pružinská et al. 2003; Kleffmann et al. 2004; Sakuraba et al. 2012b). Further characterization of PAO has shown that the enzyme is a Fe-dependent monooxygenase belonging to the Rieske-type iron-sulfur oxygenase family (Hörtensteiner et al. 1998; Gray et al. 2002; Pružinská et al. 2003). Interestingly, an additional factor, called RCC FORMING FACTOR (RFF), indispensable for PAO/RCCR activity *in vitro* has also been described (Pružinská et al. 2005). RFF could be a reactive oxygen species (ROS)-scavenging protein such as a peroxidase possibly required to remove ROS that are likely produced as by-products of PAO activity (Silvain Aubry and Stefan Hörtensteiner, unpublished data).

Suppression of PAO in *Arabidopsis*, corn (*Zea mays*), rice and tomato has been shown to induce premature cell death (Spassieva and Hille 2002; Pružinská et al. 2003; Tanaka et al. 2003; Pružinská et al. 2005; Tang et al. 2011). Stay-green and cell-death phenotypes of *Arabidopsis pao1* mutants (originally identified as *accelerated cell death 1* (*acd1*; Greenberg and Ausubel 1993)) is due to the accumulation of Pheide *a* (Pružinská et al. 2003; Tanaka et al. 2003). Surprisingly, the cell death phenotype of *PAO* mutants is not strictly connected to light, but also occurs in the dark (Pružinská et al. 2003; Pružinská et al. 2005; Hirashima et al. 2009). Thus, rather than being solely phototoxic, Pheide has been speculated to act as signaling molecule that may be exported from the

chloroplast, like suggested for Mg-protoporphyrin IX, the first intermediate of the Chl branch of the tetrapyrrole biosynthesis pathway (Mochizuki et al. 2001; Hirashima et al. 2009). However, characterization of METYHL ESTERASE (MES) 16, the enzyme demethylating FCCs in the cytosol of *Arabidopsis* (see below), revealed that an export of Pheide from the chloroplasts of *pao1* is unlikely (Christ et al. 2012). *In vitro*, MES16 can demethylate Pheide and convert it to pyroPheide but pyroPheide was not detected in *pao1*. However, when MES16 was mistargeted to the chloroplast, 75% of the Pheide accumulating in *pao1* was converted to pyroPheide (Schelbert et al. 2009; Christ et al. 2012). This finding indicates that Pheide is most probably not a chloroplast-to-nucleus retrograde signal itself but rather seems to trigger a signaling cascade involving other factors.

RCCR has originally been cloned from barley (*Hordeum vulgare*) and *Arabidopsis*, and was localized to the chloroplast (Wüthrich et al. 2000). Reduction of RCC by RCCR occurs in a stereospecific fashion, which can be different between RCCR orthologues (Mühlecker et al. 1997; Mühlecker et al. 2000). For instance, *Arabidopsis* RCCR produces *p*FCC whereas *Capsicum annuum* RCCR converts RCC into the C1-epimer of *p*FCC, *epi-p*FCC (Hörtensteiner et al. 2000). Interestingly, the *Arabidopsis* RCCR stereospecificity can be manipulated by a Phe-to-Val exchange at residue 218 (Pružinská et al. 2007). RCCR crystallisation and site-directed mutagenesis confirmed that residue 218 together with Glu154 and Asp291 are located within the substrate-binding pocket of RCCR and are required for its activity (Sugishima et al. 2009; Sugishima et al. 2010; Pattanayak et al. 2012). In contrast to senescence-related expression of *PAO*, Northern blot analysis revealed a constitutive expression of *RCCR* in leaves and roots (Wüthrich et al. 2000). Furthermore, RCCR was shown to be also targeted to the mitochondria, suggesting that RCCR could have other roles besides converting RCC to *p*FCC (Mach et al. 2001). Loss of RCCR in *Arabidopsis* causes the *acd2* phenotype, which is characterized by the spontaneous spreading of light-dependent cell death lesions during plant growth and development, and by constitutive activation of defenses in the absence of environmental stress (Mach et al. 2001; Yao and Greenberg 2006; Pružinská et al. 2007). *acd2* accumulates RCC and RCC-like pigments in the vacuole, indicating that these tetrapyrroles can move within the cell (Pružinská et al. 2007). RCC and RCC-like pigments are thought to act as signaling molecules and trigger the cell death observed in *acd2* (Mach et al. 2001; Yao and Greenberg 2006; Pattanayak et al. 2012). Part of the cascade leading to cell death in *acd2* is the loss of the mitochondrial membrane potential and mitochondrial H_2O_2 production (Yao and Greenberg 2006). Specific targeting of RCCR to the mitochondria of *acd2* dramatically reduces RCC accumulation, cell death and mitochondrial ROS

production (Pattanayak et al. 2012). This rescue effect is dependent on the activity of RCCR since a mitochondria-targeted Glu154Ala variant of RCCR did not complement the cell death phenotype of *acd2*. Collectively, these *in vivo* data on RCCR function(s) provide evidence that this enzyme is involved in protection against pro-death molecules (such as RCC) in both chloroplast and mitochondria. These pro-death molecules, substrates of RCCR, are mobile within cells and have a major effect on mitochondria (Pattanayak et al. 2012).

B.1.6 Interaction of CCEs at the thylakoid membrane

Recently, advances have been made in understanding the topology of the first steps of Chl breakdown during leaf senescence (Sakuraba et al. 2012b; Sakuraba et al. 2013). Using co-immunoprecipitation and bimolecular fluorescence complementation approaches, it has been demonstrated that SGR, NYC1, NOL, HCAR, PPH, PAO and RCCR interact at the thylakoid membrane (Fig. 2). These interactions are proposed to create an enzyme complex, which mediates channelling of phototoxic catabolites. The observation that these interactions do not occur in a *sgr* mutant suggests the possibility that SGR recruits the other CCEs at the thylakoid membrane and acts as a hub. In the model proposed by Sakuraba et al. (2012b), all these steps of Chl degradation occur at the thylakoid membrane and ultimately lead to the release of *p*FCC, the first non-phototoxic catabolite, into the stroma. SGR has been shown to specifically interact with LHCII but not with LHCI subunits, and to participate in the destabilization of the Chl-apoprotein complexes (Park et al. 2007). Existence of the same or a similar complex for Chl degradation in PSI is highly probable but has not yet been demonstrated.

B.2 Modifications of fluorescent chlorophyll catabolites

B.2.1 Diversity of colorless chlorophyll catabolites

After its release into the chloroplast stroma, non-phototoxic and colorless *p*FCC is modified by different enzymes, leading to the production of *modified* FCCs (*m*FCCs). All colorless Chl catabolites are thought to derive from *p*FCC, to be modified in both chloroplast and cytosol, and finally to be non-enzymatically isomerized and stored in the vacuole as nonfluorescent Chl catabolites (NCCs) or dioxobilin-type nonfluorescent Chl catabolites (DNCCs). Since the identification of the first NCC, *Hv*-NCC-1 in 1991 (Kräutler et al. 1991), up to 40 different colorless Chl catabolites have been structurally characterized (Table 1; Hörtensteiner 2012).

297 These catabolites are divided into four classes (FCCs, NCCs, DNCCs and YCCs; Fig. 1) depending on specific
298 modifications at several side positions of the tetrapyrrole backbone, which determine a distinct UV/Vis spectrum
299 for each class of catabolites (Fig. 3). The recently identified yellow Chl catabolites (YCCs) have been speculated
300 to originate from the oxidation of NCCs in the vacuole (Moser et al. 2008a; Scherl et al. 2012).
301
302 B.2.2 Demethylation
303
304 Demethylation of Chl catabolites at $C13^2$ is species-specific: demethylated Chl catabolites have so far only been
305 found in *Arabidopsis*, rape (*Brassica napus*) and spinach (*Spinacia oleracea*; Mühlecker and Kräutler 1996;
306 Berghold et al. 2002; Pružinská et al. 2005; Hörtensteiner and Kräutler 2011). In a recent study, *Arabidopsis*
307 MES16 was identified as the enzyme catalyzing demethylation of Chl catabolites (Christ et al. 2012). MES16
308 localizes to the cytosol and *in vivo* acts within the Chl degradation pathway on the level on FCCs but not on
309 Pheide, like suggested in previous studies that proposed pheophorbidase, a homolog of MES16, to demethylate
310 Pheide to pyroPheide in *Chenopodium album* and radish (*Raphanus sativus*; Shioi et al. 1996b; Suzuki et al.
311 2002; Suzuki et al. 2006). Notably, demethylation of FCCs accelerates their isomerization in the vacuole. As a
312 consequence, senescent leaves of *Arabidopsis mes16* mutants are fluorescent under UV light due to the vacuolar
313 accumulation of methylated FCCs. Interestingly, *mes16* mutants are not affected in Chl *a* and *b* degradation and
314 do not show any visible phenotype under controlled growth conditions.
315
316 B.2.3 Hydroxylation and glucosylation
317
318 $C8^2$ hydroxylation of *p*FCC is the only side chain modification found in all species from which colorless Chl
319 catabolites have been structurally characterized. The nature of the enzyme(s) responsible for hydroxylation is not
320 known. However, isolation of gerontoplasts from barley revealed that not only *p*FCC is produced *in organello*
321 but also a second, more polar, FCC (Matile et al. 1992). The structure of this polar FCC has not yet been
322 determined, but was speculated to be $C8^2$ hydroxy-*p*FCC and cytochromes P450 monooxygenases have been
323 suggested as possible candidates for *p*FCC hydroxylation (Matile et al. 1999). Although the majority of the 244
324 full-length P450 proteins that are encoded in the *Arabidopsis* genome are predicted to localize in the ER, some
325 P450 have been experimentally shown to be targeted to the chloroplast (Schuler et al. 2006). However, dark-
326 incubation of detached *Arabidopsis* leaves in an atmosphere containing carbon monoxide (CO), known to be an

inhibitor of cytochrome P450s, does not seem to prevent FCC hydroxylation (Christ et al. 2013). Assuming that CO can diffuse into the chloroplast, FCC hydroxylation thus appears not to be mediated by a cytochrome P450 enzyme.

In some species such as *Arabidopsis*, tobacco (*Nicotiana rustica*) and rape, the $C8^2$ hydroxyl group of FCCs appears to be subsequently malonylated and/or glucosylated (Hörtensteiner 1998; Berghold et al. 2004; Pružinská et al. 2005). The molecular nature of respective activities remains unknown, although a malonyltransferase activity has been partially purified from *Brassica napus* (Hörtensteiner, 1998). *Arabidopsis* UDP-DEPENDENT GLYCOSYLTRANSFERASES (UGTs) are known to catalyze the addition of a sugar group to hydroxyl groups of target molecules by formation of a glycosidic bond (Paquette et al. 2003; Osmani et al. 2009). Therefore, it can be imagined that one or several of the 120 cytosol-localized UGTs (Paquette et al. 2003) are responsible for the addition of glucose to $C8^2$ hydroxy-FCCs in *Arabidopsis*.

B.2.4 Deformylation

Deformylated Chl catabolites have been found in barley, Norway maple (*Acer platanoides*) and *Arabidopsis*, and are known as DNCCs (Losey and Engel 2001; Müller et al. 2011; Christ et al. 2013). NCCs and DNCCs differ at the C6 side group of pyrrole ring B, which is a formyl group in NCCs and an oxo group in DNCCs. DNCCs are the major Chl catabolites in *Arabidopsis*, accounting for more than 80% of all final Chl catabolites (Christ et al. 2013). Cytochrome P450 (CYP) CYP89A9 has recently been identified in *Arabidopsis* to be responsible for the oxidative deformylation of FCCs to dioxobilin-type FCCs (DFCCs), extending the wide substrate spectrum of CYPs (Bak et al. 2011) to linear tetrapyrroles. *cyp89a9* mutants do not produce DNCCs but accumulate proportionally higher amounts of NCCs. CYP89A9, as most CYP proteins, likely localizes to the ER membrane. Interestingly, deformylation of FCCs by CYP89A9 must precede demethylation by MES16 since demethylated catabolites are not substrates of CYP89A9, suggesting a close interaction between the ER and the chloroplast envelope (Fig. 2).

B.2.5 Hypermodification

Hypermodified FCCs (*hm*FCCs) are *m*FCCs in which the C17 propionic acid chain is conjugated with different groups such as digalactosylglycerol or daucic acid (Moser et al. 2008b; Moser et al. 2009; Banala et al. 2010; Kräutler et al. 2010; Vergeiner et al. 2013). *hm*FCCs were shown to be persistant and to accumulate in senescent leaves, because the C17 modifications inhibit their isomerization to respective NCCs (Moser et al. 2009; Vergeiner et al. 2013). Although it remains to be experimentally proven, *hm*FCCs are, like most *m*FCCs, most probably also imported into the vacuole. As a consequence of the accumulation of *hm*FCCs, ripe fruits and senescent leaves of some species such as banana (*Musa acuminate* or *Musa cavendish*) and *Spathiphyllum wallisii* are fluorescing under UV light. Interestingly, in a yellow banana fruit, more intense fluorescence than in other parts of the peel is observed around necrotic spots that first appear around stomata (Moser et al. 2009). Occurence of these highly fluorescent rings is thought to result from the conversion of *m*FCCs to specific *hm*FCCs just prior to cell death. The mechanism increasing fluorescence in the surrounding of the necrotic spots remains unknown. *De novo hm*FCCs synthesis from Chl precursors is unlikely. However, it could be due to the degradation of remaining Chl in the yellow peel of banana, although most Chl has already been broken down at this stage.

B.2.6 Isomerization of FCCs in the vacuole

*m*FCCs have been described to be converted to their respective NCCs inside the vacuole by nonenzymatic isomerization. This significantly occurs only under acidic conditions such as found in the vacuole (pH 5-6; Fig. 1 and 2; Oberhuber et al. 2003). Likewise, DFCCs produced by CYP89A9 in *Arabidopsis* through an oxidative deformylation of FCCs, were also shown to be converted to respective DNCCs at pH 5 *in vitro* (Christ et al. 2013). The rate of FCC-to-NCC isomerization increases with decreasing pH and seems to be also influenced by certain modifications of FCC side chains (Moser et al. 2009; Christ et al. 2012). Thus, *m*FCCs harbouring an intact methyl group at $C13^2$ show slower isomerization *in vitro* when compared to demethylated FCCs (Christ et al. 2012). Moreover, $C17^3$ modifications found in *hmFCC*s are thought to inhibit their conversion to *hm*NCCs (Moser et al. 2009).

B.2.7 Transport of FCCs within the cell

385 Chl degradation starts in the chloroplast and ends in the vacuole (Fig. 2). Therefore, two translocation systems
386 have to transport Chl catabolites across the chloroplast envelope and the tonoplast. A single study on Chl
387 catabolite transport across the plastid envelope showed that the release of FCCs from isolated barley
388 gerontoplasts is enhanced by external supply of ATP (Matile et al. 1992). This observation has led to the
389 hypothesis that transport of FCCs across the chloroplast envelope could be mediated by ATP BINDING
390 CASSETTE (ABC) transporter(s) (Hörtensteiner 2006). Interestingly, suppression of ABCG2, a mammalian
391 ABC-type transporter of the G subfamily, in mice triggers a porphyria-like phenotype (phototoxic ear lesions),
392 which is due to the incapacity of the animals to detoxify food-derived Pheide and protoporphyrin IX circulating
393 in the blood stream (Jonker et al. 2002). The *Arabidopsis* genome encodes 130 ABC transporters, which are
394 localized in membranes of most subcellular compartments (Kang et al. 2011a). To date, screening single and
395 multiple T-DNA insertion lines for ABCG2 homologues and other ABC-transporters that are predicted to
396 localize to the chloroplast envelope did not provide any evidence for their involvement in FCC export from the
397 chloroplast (Sylvain Aubry, Bastien Christ, Silvia Schelbert, Maja Schellenberg, Kathrin Salinger and Stefan
398 Hörtensteiner, unpublished data). Most probably, chloroplast export of FCCs and likely also of other linear
399 tetrapyrrole such as phytochromobillin is performed by several transporters. This potential redundancy increases
400 the difficulty of identifying these transporters *in vivo*.
401
402 Compared to the transport across the chloroplast envelope, import of FCCs from the cytosol to the vacuole is
403 better understood. Heterologous expression in yeast of *Arabidopsis At*ABCC2 and *At*ABCC3, two members of
404 the C subfamily of ABC transporters, revealed them to be capable of importing NCCs *in vitro* (Lu et al. 1998;
405 Tommasini et al. 1998). Although these results have been obtained using NCCs rather than FCCs as substrate,
406 this type of transporters is most probably involved in Chl catabolite transport across the tonoplast *in vivo*.
407 However, like for the export of FCCs from the chloroplast, redundancy could render their reverse genetic
408 identification difficult.
409
410 B.2.8 Storage of tetrapyrrole catabolites or further degradation?
411
412 Monopyrrolic catabolites of Chl have been shown to accumulate during leaf senescence in barley and radish
413 (Suzuki et al. 1999; Suzuki and Shioi 1999). This finding is consistent with the observation that DNCCs and
414 NCCs accumulating in senescent leaves of barley represent only a minor fraction of the total amount of Chl that

has been degraded (Kräutler et al. 1991; Losey and Engel 2001; Aditi Das and Stefan Hörtensteiner, unpublished data). By contrast, in *Arabidopsis*, quantification of DNCCs and NCCs accumulating in yellow leaves revealed that their amount reflects the Chl content of green leaves, indicating that DNCCs and NCCs are not further fragmented (Christ et al. 2013). The same observation was made in *Cercidiphyllum japonicum* (Curty and Engel 1996). Together, these studies imply that the fate of NCCs/DNCCs in the vacuole (storage or further fragmentation) differs between plant species. However, it cannot be excluded that the inconsistency between amounts of colorless catabolites and degraded Chl in some species is due to a second and entirely different pathway for Chl breakdown that may be independent of PAO activity.

B.2.9 By-products of chlorophyll breakdown

During leaf senescence, one mole of degraded Chl leads to the production of one mole of colorless catabolites. Within the chloroplast this leads to the release of magnesium and phytol as by-products (Fig. 1). Magnesium is thought to be reallocated to growing tissues together with other metal ions set free during the degradation of thylakoid components. Two main routes have been described for the fate of phytol. Free phytol can be phosphorylated to phytoldiphosphate through the sequential action of two kinases and is subsequently employed for tocopherol synthesis (Valentin et al. 2006; Ischebeck et al. 2006). Recently, characterization of the two acyltransferases PHYTYL ESTER SYNTHASE 1 and 2 provided evidence for an alternative destiny of free phytol, i.e. through fatty acid phytyl ester (FAPE) synthesis in plastoglobules (Lippold et al. 2012).

FCC modifications also lead to the formation of by-products. Even though it has not been experimentally shown, Chl catabolite demethylation (through MES16) and oxidative deformylation (through CYP89A9) are thought to produce methanol and formate, respectively (Fig. 1). In *Arabidopsis*, the amount of Chl catabolites produced during leaf senescence is about 1 µmol per gram fresh weight. Under the assumption that 100% of the Chl catabolites are demethylated and deformylated, Chl breakdown is responsible for the formation of 1 µmol each of methanol and formate per gram fresh weight, amounts that are not negligible. Methanol is known to be produced in leaves by processes such as pectin and lignin degradation and to be metabolized by C1-metabolism via production of formate or to exit the leaf via the stomata (Fall and Benson 1996; Igamberdiev et al. 1999; Gout et al. 2000). Although stomata are thought to remain open during the late stages of senescence (Zhang and Gan 2012), it can still be imagined that Chl-derived methanol may partially accumulate within the leaves and

have physiological effects. Indeed, in rice, methanol formation during leaf senescence has been connected to an increase in tryptophan biosynthesis that involves the transcription factor WRKY14 (Kang et al. 2011b). Tryptophan biosynthesis has been shown to promote serotonin production, which in turn delays leaf senescence (Kang et al. 2009). Furthermore, exogenous application of methanol modulates the expression of hundreds of genes involved in multiple detoxification and signaling pathways (Downie et al. 2004). Although a regulatory role of methanol during senescence in *Arabidopsis* has not been established, it may be interesting to investigate the contribution of Chl catabolite demethylation to the total production of methanol during leaf senescence. However, the possibility that FCC demethylation may indirectly regulate gene expression is rather unlikely, because *mes16* mutants do not show any accelerated or delayed leaf senescence phenotype.

In leaves, formate is known to be the by-product of photorespiration and fermentation pathways, and possibly the product of direct CO_2 reduction in chloroplasts (Igamberdiev et al. 1999). As mentioned above, formate could also be formed from methanol generated by pectin and lignin degradation, and potentially also by FCC demethylation. In theory, FCC-to-DFCC conversion by CYP89A9 should also contribute to the formation of formate in senescent leaves. Because formate is less volatile than methanol, it has to be metabolized within senescing leaves. Two routes for formate utilization have been described in plants (Igamberdiev et al. 1999). The first one is mediated by FORMATE DEHYDROGENASE (FDH) which converts formate to CO_2 (Li et al. 2000; Olson et al. 2000). Although overexpression of FDH in *Arabidopsis* has been shown to increase tolerance to exogenous application of formate, the role of FDH in leaves remains unknown (Li et al. 2002). Transcriptome coexpression analysis using ATTED-II (Obayashi et al. 2009) reveals that *Arabidopsis* FDH is co-expressed with CCEs, indicating that the enzyme could have a role during leaf senescence. To the best of our knowledge, accumulation of formate in *fdh* mutants has never been reported in the literature. Furthermore, *Arabidopsis fdh* mutants do not show any accumulation of formate during dark-induced leaf senescence (Bastien Christ and Stefan Hörtensteiner, unpublished data). The non-accumulation of formate in *fdh* mutants could arise from a compensation effect of a second route of formate utilization. Indeed, formate can be condensed with tetrahydrofolate (THF) to produce formyl-THF by the action of 10-FORMYL-THF SYNTHETASE (THFS; Igamberdiev et al. 1999). Formyl-THF is then further used for serine and methionine biosynthesis. In *Arabidopsis*, THFS is encoded by a single copy gene but has not been analyzed so far.

C. SIGNIFICANCE OF CHLOROPHYLL BREAKDOWN

C.1 Detoxification and nutrient remobilization

After the onset of senescence, leaves undergo complex changes that should be seen as "transdifferentiation" rather than as "deterioration" processes (Thomas et al., 2003). Recycling and detoxification of (macro-) molecules are indeed the consequences of structural and biochemical changes occurring during leaf senescence. Disintegration of cellular components is mediated through fine-tuned catabolic as well as anabolic steps that reduce deleterious effects of intermediates of degradation and maximize nutrient remobilization (e.g. nitrogen, phosphorus, sulphur, minerals, metals ions and carbon skeletons). Chl breakdown is a direct prerequisite for the remobilization of chloroplast lipids, proteins and metals. This fact is highlighted by the effect of the suppression of enzymes involved in Chl breakdown such as PAO or RCCR (see above), which lead to the accumulation of toxic Chl intermediates and, thus, to early cell death phenotypes. Although it has not yet been precisely characterized, these mutants seem to be also affected in the ability to remobilize nutrients and consequently show a low germination rate. In addition, it has been demonstrated in *Arabidopsis* that the suppression of Chl *b* to *a* conversion, which leads to Chl retention in cotyledons during seed drying, dramatically decreases seed germination capacity (Nakajima et al. 2012).

C.2 Protection against pathogens

Several lines of evidence suggest that (partial) degradation of Chl is involved in the response of plants against pathogens. SGR appears to be necessary for the development of chlorosis upon infection of *Arabidopsis* with *Pseudomonas syringae* pv *tomato* (Mecey et al. 2011). Similarly, levels of SGR in silencing or overexpressing *Arabidopsis* lines correlate with the severeness of the hypersensitive response triggered upon *P. syringae* infection (Mur et al. 2010). Moreover, *At*CLH1 was proposed to be involved in pathogen responses (Kariola et al. 2005). Silencing of *At*CLH1 was shown to alter resistance or susceptibility of plants towards two different types of necrotrophic pathogens, *Erwinia carotovora* and *Alternaria brassicicola*. Absence of CLH1, which is thought to degrade Chl in damaged tissue, was connected with ROS production during necrotrophic pathogen attack, which in turn would activate and inactivate salicylic acid-dependent and jasmonic acid-dependent responses, respectively (Kariola et al. 2005). However, this model for CLH function during pathogen attack is

505 based on indirect observations and has to be considered with caution. Together, these studies suggest that Chl
506 breakdown enzymes and catabolites could play an important role during pathogen infection.
507
508 C.3 Putative role(s) of FCC modifications
509
510 Retention of FCCs in *mes16* mutants and lack of DNCC formation in *cyp89a9* mutants does not seem to affect
511 plant growth and/or leaf senescence, i.e. no phenotype was observed in *mes16, cyp89a9* and *mes16 cyp89a9*
512 mutants during vegetative growth, and Chl *a* and *b* degradation during leaf senescence was indistinguishable
513 from wild-type plants (Christ et al. 2012; Christ et al. 2013). Thus, the role(s) of FCC modification remain(s)
514 unclear. One hypothesis is that FCC modification could participate in the detoxification of Chl catabolites. The
515 first steps of degradation produce phototoxic catabolites and FCC modifications could lead to further decrease of
516 the light absorption capacities of the catabolites (Fig. 4). Indeed, demethylation of FCCs increases the rate of
517 isomerization to nonfluorescent catabolites and, thus, facilitates the loss of their 360 nm absorption peak.
518 Furthermore, DFCC formation by CYP89A9 results in the loss of the C5-formyl group of FCCs and,
519 consequently, of the 320 nm absorption peak. One reason for the absence of any phenotype in *mes16* and
520 *cyp89a9* mutants could be the fact that in controlled experimental facilities these mutants are grown under UV-
521 limited conditions. It can be speculated that, during senescence under sun-light conditions, plants could be
522 affected if colorless Chl catabolites are retained that absorb light between 300 and 380 nm. This hypothesis
523 could be tested by growing the mutants under natural or artificial UV-B-containing light conditions.
524
525 Besides reducing the light absorption capacity of colorless Chl catabolites, modifications of FCC side chains
526 increase their polarity (Fig. 1). This observation corroborates the idea that FCC modification directly contributes
527 to Chl catabolite detoxification. Indeed, sequential hydroxylation and glucosylation steps are known to
528 participate in the detoxification of various molecules such as xenobiotics by increasing their polarity (Pedras et
529 al. 2001; Dosnon-Olette et al. 2011). Therefore, an increase in the solubility of the catabolites likely facilitates
530 the relocation of FCCs from the chloroplast to the vacuole. Identification of the enzyme(s) responsible for FCC
531 hydroxylation, together with the knowledge on FCC demethylation and oxidative deformylation could help
532 testing if FCC modification has indeed a physiological role. It would be of interest to study leaf senescence in
533 *Arabidopsis* plants that are deficient in all FCC modifying activities and would thus accumulate only *p*FCC and
534 *p*NCC during Chl breakdown.

Why do FCC modifications occur in a species-specific manner (see Table 1)? One hypothesis is that FCCs could have ecological functions. On one hand, plants such as *Arabidopsis* appear to avoid FCC accumulation. On the other hand, permanent FCC accumulation has been shown to occur in leaves and fruits of banana and other related taxa (Moser et al. 2009; Kräutler et al. 2010; Hörtensteiner and Kräutler 2011; Vergeiner et al. 2013). Furthermore, while humans are not overly sensitive to blue light between 400-500 nm, other animals, such as insects, are known to possess blue photoreceptors having a maximal sensitivity around 450 nm (Briscoe and Chittka 2001). It is therefore reasonable to assume that some insects are able to detect the blue fluorescence emitted by FCCs around 450 nm. In the case of plant species such as banana that naturally retain FCCs these fluorescent catabolites may play a role in beneficial interactions with insects such as pollinations or may be a signal of fruit ripening for bigger animals contributing to seed dispersal. Other plant species may benefit from the further conversion of FCCs into NCCs/DNCCs because herbivores might be able to link FCC fluorescence of senescent leaves with reduced plant fitness at this late developmental stage. Thus, by facilitating FCC-to-NCC isomerization, MES16 could, for instance, help avoiding the attraction of herbivores by the plant during nutrient relocation and seed maturation. *Arabidopsis* mutants that accumulate different relative FCC amounts during senescence (*mes16*, *mes16 cyp89a9*; Christ et al. 2012; Christ et al. 2013) could be used in future experiments to investigate if insects can indeed detect FCC fluorescence.

D. FUTURE PERSPECTIVES

Delaying the onset of leaf senescence has been described as a good strategy for increasing crop productivity (Thomas and Howarth 2000). Indeed, the yield record in corn was obtained with functional stay-green mutants. Though, suppression of Chl degradation only leads to cosmetic stay-green and/or cell-death phenotypes, which do not increase plant fitness but rather accelerate cell death and decrease seed germination. Nonetheless, understanding Chl breakdown during leaf senescence, fruit ripening and other developmental processes or stress responses is not only of interest to increase our fundamental knowledge, but it can also improve post-harvest storage. Indeed, loss of the green color due to senescence in vegetables such as broccoli (*Brassica oleracea*) decreases their commercial value. Besides open questions about FCC modifications and transport, several other aspects of Chl breakdown by the PAO pathway need further investigation. For instance, although SGR and CCEs have been shown to interact with LHCII subunits and SGR has been implicated in the destabilization of

565 Chl-apoprotein complexes during senescence, its mechanism of action remains to be defined. Furthermore, it is
566 unknown if the same mechanism is involved in the degradation of Chl from PSI. It cannot be excluded that PSI
567 degradation (partially) differs from the one of PSII. Recent studies, showing that SGR has other functions
568 besides Chl breakdown could be helpful to better understand the role(s) of this protein. The mechanism involved
569 in Chl demetalation also remains unknown. Whether it involves an MRP, MCS and/or simple changes in the pH
570 of the chloroplast stroma still needs to be demonstrated. The *in vivo* role of CLHs, proteins that are highly active
571 on Chl *in vitro*, is still unclear. A collective consideration of key studies on CLHs points to their involvement
572 during stress responses against various biotic and abiotic stresses, and not during age-dependent leaf senescence.
573
574 Chl degradation is a highly controlled process. This is seen by protein-protein interactions during the first steps
575 of the pathway that allow metabolic channelling of phototoxic catabolites (Sakuraba et al. 2012b; Sakuraba et al.
576 2013) and by the high co-regulation of Chl catabolic gene expression. However, the mechanism(s) of
577 transcriptional regulation of Chl breakdown remain(s) unknown. Interestingly, overexpression of a single CCE
578 results in an increased rate of degradation in the whole pathway (Sakuraba et al. 2012b). Finally, another very
579 interesting research area in Chl breakdown is to better understand how cell death is triggered by the
580 accumulation of Chl catabolites in mutant such as *acd1* and *acd2*. Interestingly, cell death in neither mutant is
581 mediated through a singlet oxygen signaling pathway involving EXECUTER proteins (Wagner et al. 2004) and
582 therefore seems to involve different, unknown mechanisms (Pattanayak et al. 2012; Stefan Hörtensteiner,
583 unpublished data).
584
585 ACKNOWLEDGEMENTS
586
587 This work on chlorophyll breakdown was financially supported by grants from the Swiss National Science
588 Foundation, the National Center of Competence in Research Plant Survival, a research program of the Swiss
589 National Science Foundation, and CropLife, an European FP7 Marie-Curie Initial Training Network project.
590
591

592 REFERENCES

593

594 Armstead I, Donnison I, Aubry S, et al. (2007) Cross-species identification of Mendel's I locus. Science 315:73.

595 Aubry S, Mani J, Hörtensteiner S (2008) Stay-green protein, defective in Mendel's green cotyledon mutant, acts
596 independent and upstream of pheophorbide *a* oxygenase in the chlorophyll catabolic pathway. Plant
597 Mol Biol 67:243–256.

598 Azoulay-Shemer T, Harpaz-Saad S, Cohen-Peer R, et al. (2011) Dual N- and C-terminal processing of citrus
599 chlorophyllase precursor within the plastid membranes leads to the mature enzyme. Plant Cell Physiol
600 52:70–83.

601 Bak S, Beisson F, Bishop G, et al. (2011) Cytochromes P450. The Arabidopsis Book 9:e0144

602 Banala S, Moser S, Müller T, et al. (2010) Hypermodified fluorescent chlorophyll catabolites: source of blue
603 luminescence in senescent leaves. Angew Chem Int Ed 49:5174–5177.

604 Barrett J, Jeffrey SW (1964) Chlorophyllase and formation of an atypical chlorophyllide in marine algae. Plant
605 Physiol 39:44–47.

606 Barry CS, McQuinn RP, Chung MY, et al. (2008) Amino acid substitutions in homologs of the STAY-GREEN
607 protein are responsible for the green-flesh and chlorophyll retainer mutations of tomato and pepper.
608 Plant Physiol Biochem 147:179–187.

609 Benedetti CE, Arruda P (2002) Altering the expression of the chlorophyllase gene ATHCOR1 in transgenic
610 *Arabidopsis* caused changes in the chlorophyll-to-chlorophyllide ratio. Plant Physiol 128:1255–1263.

611 Berghold J, Breuker K, Oberhuber M, et al. (2002) Chlorophyll breakdown in spinach: on the structure of five
612 nonfluorescent chlorophyll catabolites. Photosynth Res 74:109–119.

613 Berghold J, Eichmüller C, Hörtensteiner S, Kräutler B (2004) Chlorophyll breakdown in tobacco: on the
614 structure of two nonfluorescent chlorophyll catabolites. Chem Biodivers 1:657–668.

615 Berghold J, Müller T, Ulrich M, et al. (2006) Chlorophyll breakdown in maize: on the structure of two
616 nonfluorescent chlorophyll catabolites. Monatsh Chem 137:751–763.

617 Brandis A, Vainstein A, Goldschmidt EE (1996) Distribution of chlorophyllase among components of
618 chloroplast membranes in *Citrus sinensis* organs. Plant Physiol Biochem 34:49–54.

619 Briscoe AD, Chittka L (2001) The evolution of color vision in insects. Annu Rev Entomol 46:471–510.

620 Büchert AM, Civello PM, Martínez GA (2011) Characterization of Mg-dechelating substance in senescent and
621 pre-senescent *Arabidopsis thaliana* leaves. Biol Plant 55:75–82.

622 Christ B, Schelbert S, Aubry S, et al. (2012) MES16, a member of the methylesterase protein family, specifically
623 demethylates fluorescent chlorophyll catabolites during chlorophyll breakdown in *Arabidopsis*. Plant
624 Physiol 158:628–641.

625 Christ B, Süssenbacher I, Moser S, et al. (2013) Cytochrome P450 CYP89A9 is involved in the formation of
626 major chlorophyll catabolites during leaf senescence in *Arabidopsis*. Plant Cell 25:1868–1880.

627 Curty C, Engel N (1996) Detection, isolation and structure elucidation of a chlorophyll a catabolite from
628 autumnal senescent leaves of *Cercidiphyllum japonicum*. Phytochemistry 42:1531–1536.

629 Dosnon-Olette R, Schröder P, Bartha B, et al. (2011) Enzymatic basis for fungicide removal by *Elodea*
630 *canadensis*. Environ Sci Pollut Res 18:1015–1021.

631 Downie A, Miyazaki S, Bohnert H, et al. (2004) Expression profiling of the response of *Arabidopsis thaliana* to
632 methanol stimulation. Phytochemistry 65:2305–2316.

633 Fall R, Benson AA (1996) Leaf methanol — the simplest natural product from plants. Trends Plant Sci 1:296–
634 301.

635 Feller U, Anders I, Mae T (2008) Rubiscolytics: fate of Rubisco after its enzymatic function in a cell is
636 terminated. J Exp Bot 59:1615–1624.

637 Ginsburg S, Matile P (1993) Identification of catabolites of chlorophyll porphyrin in senescent rape cotyledons.
638 Plant Physiol 102:521–527.

639 Ginsburg S, Schellenberg M, Matile P (1994) Cleavage of chlorophyll-porphyrin. Requirement for reduced
640 ferredoxin and oxygen. Plant Physiol 105:545–554.

641 Gout E, Aubert S, Bligny R, et al. (2000) Metabolism of methanol in plant cells. Carbon-13 nuclear magnetic
642 resonance studies. Plant Physiol 123:287–296.

643 Gray J, Janick-Bruckner D, Bruckner B, et al. (2002) Light-dependent death of maize *lls1* cells is mediated by
644 mature chloroplasts. Plant Physiol 130:1894–1907.

645 Greenberg JT, Ausubel FM (1993) *Arabidopsis* mutants compromised for the control of cellular damage during
646 pathogenesis and aging. Plant J 4:327–341.

647 Harpaz-Saad S, Azoulay T, Arazi T, et al. (2007) Chlorophyllase is a rate-limiting enzyme in chlorophyll
648 catabolism and is posttranslationally regulated. Plant Cell 19:1007–1022.

649 Hirashima M, Satoh S, Tanaka R, Tanaka A (2006) Pigment shuffling in antenna systems achieved by
650 expressing prokaryotic chlorophyllide a oxygenase in *Arabidopsis*. J Biol Chem 281:15385–15393.

651 Hirashima M, Tanaka R, Tanaka A (2009) Light-independent cell death induced by accumulation of
652 pheophorbide *a* in *Arabidopsis thaliana*. Plant Cell Physiol 50:719–729.

653 Holden M (1961) The breakdown of chlorophyll by chlorophyllase. Biochem J 78:359–364.

654 Horie Y, Ito H, Kusaba M, et al. (2009) Participation of chlorophyll b reductase in the initial step of the
655 degradation of light-harvesting chlorophyll *a*/*b*-protein complexes in *Arabidopsis*. J Biol Chem
656 284:17449–17456.

657 Hörtensteiner S (2009) Stay-green regulates chlorophyll and chlorophyll-binding protein degradation during
658 senescence. Trends Plant Sci 14:155–162.

659 Hörtensteiner S (2006) Chlorophyll degradation during senescence. Annu Rev Plant Biol 57:55–77.

660 Hörtensteiner S (1998) NCC malonyltransferase catalyses the final step of chlorophyll breakdown in rape
661 (*Brassica napus*). Phytochemistry 49:953–956.

662 Hörtensteiner S (2012) Update on the biochemistry of chlorophyll breakdown. Plant Mol Biol 1–13.

663 Hörtensteiner S, Feller U (2002) Nitrogen metabolism and remobilization during senescence. J Exp Bot 53:927–
664 937.

665 Hörtensteiner S, Kräutler B (2011) Chlorophyll breakdown in higher plants. Biochim Biophys Acta 1807:977–
666 988.

667 Hörtensteiner S, Rodoni S, Schellenberg M, et al. (2000) Evolution of chlorophyll degradation: the significance
668 of RCC reductase. Plant Biol 2:63–67.

669 Hörtensteiner S, Vicentini F, Matile P (1995) Chlorophyll breakdown in senescent cotyledons of rape, *Brassica*
670 *napus* L.: enzymatic cleavage of phaeophorbide *a* in vitro. New Phytol 129:237–246.

671 Hörtensteiner S, Wüthrich KL, Matile P, et al. (1998) The key step in chlorophyll breakdown in higher plants.
672 Cleavage of pheophorbide *a* macrocycle by a monooxygenase. J Biol Chem 273:15335–15339.

673 Igamberdiev AU, Bykova NV, Kleczkowski LA (1999) Origins and metabolism of formate in higher plants.
674 Plant Physiol Biochem 37:503–513.

675 Ischebeck T, Zbierzak AM, Kanwischer M, Dörmann P (2006) A salvage pathway for phytol metabolism in
676 *Arabidopsis*. J Biol Chem 281:2470–2477.

677 Iturraspe J, Moyano N, Frydman B (1995) A new 5-formylbilinone as the major chlorophyll a catabolite in tree
678 senescent leaves. J Org Chem 60:6664–6665.

679 Jakob-Wilk D, Holland D, Goldschmidt EE, et al. (1999) Chlorophyll breakdown by chlorophyllase: isolation
680 and functional expression of the Chlase1 gene from ethylene-treated *Citrus* fruit and its regulation
681 during development. Plant J 20:653–661.

682 Jiang H, Li M, Liang N, et al. (2007) Molecular cloning and function analysis of the stay green gene in rice.
683 Plant J 52:197–209.

684 Jonker JW, Buitelaar M, Wagenaar E, et al. (2002) The breast cancer resistance protein protects against a major
685 chlorophyll-derived dietary phototoxin and protoporphyria. Proc Natl Acad Sci U S A 99:15649–15654.

686 Kang J, Park J, Choi H, et al. (2011a) Plant ABC transporters. The Arabidopsis Book 9:e0153.

687 Kang K, Kim Y-S, Park S, Back K (2009) Senescence-induced serotonin biosynthesis and its role in delaying
688 senescence in rice leaves. Plant Physiol 150:1380–1393.

689 Kang K, Park S, Natsagdorj U, et al. (2011b) Methanol is an endogenous elicitor molecule for the synthesis of
690 tryptophan and tryptophan-derived secondary metabolites upon senescence of detached rice leaves.
691 Plant J 66:247–257.

692 Kariola T, Brader G, Li J, Palva ET (2005) Chlorophyllase 1, a damage control enzyme, affects the balance
693 between defense pathways in plants. Plant Cell 17:282–294.

694 Kleffmann T, Russenberger D, von Zychlinski A, et al. (2004) The *Arabidopsis thaliana* chloroplast proteome
695 reveals pathway abundance and novel protein functions. Curr Biol 14:354–362.

696 Kräutler B, Banala S, Moser S, et al. (2010) A novel blue fluorescent chlorophyll catabolite accumulates in
697 senescent leaves of the peace lily (*Spathiphyllum wallisii*) and indicates a divergent path of chlorophyll
698 breakdown. FEBS Lett 584:4215–4221.

699 Kräutler B, Jaun B, Bortlik K-H, et al. (1991) On the enigma of chlorophyll degradation: the constitution of a
700 secoporphinoid catabolite. Angew Chem Int Ed 30:1315–1318.

701 Kusaba M, Ito H, Morita R, et al. (2007) Rice NON-YELLOW COLORING1 is involved in light-harvesting
702 complex II and grana degradation during leaf senescence. Plant Cell 19:1362–1375.

703 Li R, Moore M, Bonham-Smith PC, King J (2002) Overexpression of formate dehydrogenase in *Arabidopsis*
704 *thaliana* resulted in plants tolerant to high concentrations of formate. J Plant Physiol 159:1069–1076.

705 Li R, Ziola B, King J (2000) Purification and characterization of formate dehydrogenase from *Arabidopsis*
706 *thaliana*. J Plant Physiol 157:161–167.

707 Lippold F, Dorp K vom, Abraham M, et al. (2012) Fatty acid phytyl ester synthesis in chloroplasts of
708 *Arabidopsis*. Plant Cell 24:2001–2014.

709 Losey FG, Engel N (2001) Isolation and characterization of a urobilinogenoidic chlorophyll catabolite from
710 *Hordeum vulgare* L. J Biol Chem 276:27233–27236.

711 Lu Y-P, Li Z-S, Drozdowicz Y-M, et al. (1998) AtMRP2, an *Arabidopsis* ATP binding cassette transporter able
712 to transport glutathione S-conjugates and chlorophyll catabolites: functional comparisons with
713 AtMRP1. Plant Cell 10:267–282.

714 Lundquist PK, Poliakov A, Bhuiyan NH, et al. (2012) The functional network of the *Arabidopsis* plastoglobule
715 proteome based on quantitative proteomics and genome-wide coexpression analysis. Plant Physiol
716 158:1172–1192.

717 Luo Z, Zhang J, Li J, et al. (2013) A STAY-GREEN protein SlSGR1 regulates lycopene and β-carotene
718 accumulation by interacting directly with SlPSY1 during ripening processes in tomato. New Phytol
719 198(2):442–452.

720 Mach JM, Castillo AR, Hoogstraten R, Greenberg JT (2001) The *Arabidopsis*-accelerated cell death gene *ACD2*
721 encodes red chlorophyll catabolite reductase and suppresses the spread of disease symptoms. Proc Natl
722 Acad Sci U S A 98:771–776.

723 Makino A, Osmond B (1991) Effect of nitrogen nutrition on nitrogen partitioning between chloroplasts and
724 mitochondria in pea and wheat. Plant Physiol 96:355–362.

725 Matile P, Hörtensteiner S, Thomas H (1999) Chlorophyll degradation. Annu Rev Plant Physiol Plant Mol Biol
726 50:67–95.

727 Matile P, Hörtensteiner S, Thomas H, Kräutler B (1996) Chlorophyll breakdown in senescent leaves. Plant
728 Physiol 112:1403–1409.

729 Matile P, Schellenberg M, Peisker C (1992) Production and release of a chlorophyll catabolite in isolated
730 senescent chloroplasts. Planta 187:230–235.

731 Matile P, Schellenberg M, Vicentini F (1997) Localization of chlorophyllase in the chloroplast envelope. Planta
732 201:96–99.

733 Mayer H (1930) Untersuchungen über die Chlorophyllase. Planta 11:294–330.

734 Mecey C, Hauck P, Trapp M, et al. (2011) A critical role of STAYGREEN/Mendel's I locus in controlling
735 disease symptom development during *Pseudomonas syringae* pv *tomato* infection of *Arabidopsis*. Plant
736 Physiol 157:1965–1974.

737 Meguro M, Ito H, Takabayashi A, et al. (2011) Identification of the 7-hydroxymethyl chlorophyll a reductase of
738 the chlorophyll cycle in *Arabidopsis*. Plant Cell 23:3442–3453.

739 Mendel G (1866) Versuche über Pflanzenhybriden. Verh Naturforsch Ver Brünn 4:3–47.

740 Mochizuki N, Brusslan JA, Larkin R, et al. (2001) *Arabidopsis genomes uncoupled 5* (GUN5) mutant reveals the
741 involvement of Mg-chelatase H subunit in plastid-to-nucleus signal transduction. Proc Natl Acad Sci U
742 S A 98:2053–2058.

743 Morita R, Sato Y, Masuda Y, et al. (2009) Defect in non-yellow coloring 3, an α/β hydrolase-fold family protein,
744 causes a stay-green phenotype during leaf senescence in rice. Plant J 59:940–952.

745 Moser S, Aarts M, Müller T, Kräutler B (2008a) A yellow chlorophyll catabolite is a pigment of the fall colours.
746 Photochem Photobiol Sci 7:1577–1581.

747 Moser S, Müller T, Ebert MO, et al. (2008b) Blue luminescence of ripening bananas. Angew Chem Int Ed
748 47:8954–8957.

749 Moser S, Müller T, Holzinger A, et al. (2009) Fluorescent chlorophyll catabolites in bananas light up blue halos
750 of cell death. Proc Natl Acad Sci U S A 106:15538–15543.

751 Mühlecker W, Kräutler B (1996) Breakdown of chlorophyll: constitution of nonfluorescing chlorophyll-
752 catabolites from senescent cotyledons of the dicot rape. Plant Physiol Biochem 34:61–75.

753 Mühlecker W, Kräutler B, Moser D, et al. (2000) Breakdown of chlorophyll: a fluorescent chlorophyll catabolite
754 from sweet pepper (*Capsicum annuum*). Helv Chim Acta 83:278–286.

755 Mühlecker W, Ongania K-H, Kräutler B, et al. (1997) Tracking down chlorophyll breakdown in plants:
756 elucidation of the constitution of a "fluorescent" chlorophyll catabolite. Angew Chem Int Ed 36:401–
757 404.

758 Müller T, Moser S, Ongania K-H, et al. (2006) A divergent path of chlorophyll breakdown in the model plant
759 *Arabidopsis thaliana*. ChemBioChem 7:40–42.

760 Müller T, Rafelsberger M, Vergeiner C, Kräutler B (2011) A dioxobilane as product of a divergent path of
761 chlorophyll breakdown in Norway maple. Angew Chem Int Ed 50:10724–10727.

762 Müller T, Ulrich M, Ongania KH, Kräutler B (2007) Colorless tetrapyrrolic chlorophyll catabolites found in
763 ripening fruit are effective antioxidants. Angew Chem Int Ed 46:8699–8702.

764 Mur LAJ, Aubry S, Mondhe M, et al. (2010) Accumulation of chlorophyll catabolites photosensitizes the
765 hypersensitive response elicited by *Pseudomonas syringae* in *Arabidopsis*. New Phytol 188:161–174.

766 Nakajima S, Ito H, Tanaka R, Tanaka A (2012) Chlorophyll *b* reductase plays an essential role in maturation and
767 storability of *Arabidopsis* seeds. Plant Physiol 160:261–273.

768 Obayashi T, Hayashi S, Saeki M, et al. (2009) ATTED-II provides coexpressed gene networks for *Arabidopsis*.
769 Nucleic Acids Res 37:D987–D991.

770 Oberhuber M, Berghold J, Breuker K, et al. (2003) Breakdown of chlorophyll: a nonenzymatic reaction accounts
771 for the formation of the colorless "nonfluorescent" chlorophyll catabolites. Proc Natl Acad Sci U S A
772 100:6910–6915.

773 Oberhuber M, Berghold J, Mühlecker W, et al. (2001) Chlorophyll breakdown - on a nonfluorescent chlorophyll
774 catabolite from spinach. Helv Chim Acta 84:2615–2627.

775 Olson, Skavdahl, Ramberg, et al. (2000) Formate dehydrogenase in *Arabidopsis thaliana*: characterization and
776 possible targeting to the chloroplast. Plant Sci 159:205–212.

777 Osmani SA, Bak S, Møller BL (2009) Substrate specificity of plant UDP-dependent glycosyltransferases
778 predicted from crystal structures and homology modeling. Phytochemistry 70:325–347.

779 Paquette S, Møller BL, Bak S (2003) On the origin of family 1 plant glycosyltransferases. Phytochemistry
780 62:399–413.

781 Park S-Y, Yu J-W, Park J-S, et al. (2007) The senescence-induced STAYGREEN protein regulates chlorophyll
782 degradation. Plant Cell 19:1649–1664.

783 Pattanayak GK, Venkataramani S, Hortensteiner S, et al. (2012) ACCELERATED CELL DEATH 2 suppresses
784 mitochondrial oxidative bursts and modulates cell death in *Arabidopsis*. Plant J 69:589–600.

785 Pedras MSC, Zaharia IL, Gai Y, et al. (2001) In planta sequential hydroxylation and glycosylation of a fungal
786 phytotoxin: avoiding cell death and overcoming the fungal invader. Proc Natl Acad Sci U S A 98:747–
787 752.

788 Peoples MB, Dalling MJ (1988) The interplay between proteolysis and amino acid metabolism during
789 senescence and nitrogen allocation. In: Noodén LD, Leopold AC (eds) Senescence Aging Plants.
790 Academic Press, San Diego, USA, pp 181–217

791 Pružinská A, Anders I, Aubry S, et al. (2007) In vivo participation of red chlorophyll catabolite reductase in
792 chlorophyll breakdown. Plant Cell 19:369–387.

793 Pružinská A, Anders I, Tanner G, et al. (2003) Chlorophyll breakdown: pheophorbide *a* oxygenase is a Rieske-
794 type iron-sulfur protein, encoded by the accelerated cell death 1 gene. Proc Natl Acad Sci U S A
795 100:15259–15264.

796 Pružinská A, Tanner G, Aubry S, et al. (2005) Chlorophyll breakdown in senescent *Arabidopsis* leaves:
797 characterization of chlorophyll catabolites and of chlorophyll catabolic enzymes involved in the
798 degreening reaction. Plant Physiol 139:52–63.

799 Ren G, An K, Liao Y, et al. (2007) Identification of a novel chloroplast protein AtNYE1 regulating chlorophyll
800 degradation during leaf senescence in *Arabidopsis*. Plant Physiol 144:1429–1441.

801 Ren GD, Zhou Q, Wu SX, et al. (2010) Reverse genetic identification of CRN1 and its distinctive role in
802 chlorophyll degradation in *Arabidopsis*. J Integr Plant Biol 52:496–504.

803 Rodoni S, Mühlecker W, Anderl M, et al. (1997) Chlorophyll breakdown in senescent chloroplasts. Cleavage of
804 pheophorbide *a* in two enzymic steps. Plant Physiol 115:669–676.

805 Saga Y, Tamiaki H (2012) Demetalation of chlorophyll pigments. Chem Biodivers 9:1659–1683.

806 Sakuraba Y, Balazadeh S, Tanaka R, et al. (2012a) Overproduction of Chl *b* retards senescence through
807 transcriptional reprogramming in *Arabidopsis*. Plant Cell Physiol 53:505–517.

808 Sakuraba Y, Kim Y-S, Yoo S-C, et al. (2013) 7-Hydroxymethyl chlorophyll a reductase functions in metabolic
809 channeling of chlorophyll breakdown intermediates during leaf senescence. Biochem Biophys Res
810 Commun 430:32–37.

811 Sakuraba Y, Schelbert S, Park SY, et al. (2012b) STAY-GREEN and chlorophyll catabolic enzymes interact at
812 light-harvesting complex II for chlorophyll detoxification during leaf senescence in *Arabidopsis*. Plant
813 Cell 24:507–18.

814 Sakuraba Y, Yokono M, Akimoto S, et al. (2010) Deregulated chlorophyll *b* synthesis reduces the energy
815 transfer rate between photosynthetic pigments and induces photodamage in *Arabidopsis thaliana*. Plant
816 Cell Physiol 51:1055–1065.

817 Sato Y, Moria R, Katsuma S, et al. (2009) Two short-chain dehydrogenase/reductases, NON-YELLOW
818 COLORING 1 and NYC1-LIKE, are required for chlorophyll *b* and light-harvesting complex II
819 degradation during senescence in rice. Plant J 57:120–131.

820 Scheer H (2006) An overview of chlorophylls and bacteriochlorophylls: biochemistry, biophysics, functions and
821 applications. In: Grimm B, Porra R, Rüdiger W, Scheer H (eds) Chlorophylls Bacteriochlorophylls.
822 Biochemistry, Biophysics, Functions and Applications, Springer, Dordrecht, The Netherlands, pp 1–26

823 Schelbert S, Aubry S, Burla B, et al. (2009) Pheophytin pheophorbide hydrolase (pheophytinase) is involved in
824 chlorophyll breakdown during leaf senescence in *Arabidopsis*. Plant Cell 21:767–785

825 Schellenberg M, Matile P, Thomas H (1990) Breakdown of chlorophyll in chloroplasts of senescent barley
826 leaves depends on ATP. J Plant Physiol 136:564–568.

827 Schellenberg M, Matile P, Thomas H (1993) Production of a presumptive chlorophyll catabolite in vitro:
828 requirement for reduced ferredoxin. Planta 191:417–420.

829 Schenk N, Schelbert S, Kanwischer M, et al. (2007) The chlorophyllases AtCLH1 and AtCLH2 are not essential
830 for senescence-related chlorophyll breakdown in *Arabidopsis thaliana*. FEBS Lett 581:5517–5525.

831 Scherl M, Müller T, Kräutler B (2012) Chlorophyll catabolites in senescent leaves of the lime tree (*Tilia*
832 *cordata*). Chem Biodivers 9:2605–2617.

833 Schuler MA, Duan H, Bilgin M, Ali S (2006) *Arabidopsis* cytochrome P450s through the looking glass: a
834 window on plant biochemistry. Phytochem Rev 5:205–237.

835 Shimoda Y, Ito H, Tanaka A (2012) Conversion of chlorophyll *b* to chlorophyll *a* precedes magnesium
836 dechelation for protection against necrosis in *Arabidopsis*. Plant J 72:501–511.

837 Shioi Y, Tomita N, Tsuchiya T, Takamiya K (1996a) Conversion of chlorophyllide to pheophorbide by Mg-
838 dechelating substance in extracts of *Chenopodium album*. Plant Physiol Biochem 34:41–47.

839 Shioi Y, Watanabe K, Takamiya K (1996b) Enzymatic conversion of pheophorbide *a* to a precursor of
840 pyropheophorbide *a* in leaves of Chenopodium album. Plant Cell Physiol 37:1143–1149.

841 Spassieva S, Hille J (2002) A lesion mimic phenotype in tomato obtained by isolating and silencing an *Lls1*
842 homologue. Plant Sci 162:543–549.

843 Sugishima M, Kitamori Y, Noguchi M, et al. (2009) Crystal structure of red chlorophyll catabolite reductase:
844 enlargement of the ferredoxin-dependent bilin reductase family. J Mol Biol 389:376–387.

845 Sugishima M, Okamoto Y, Noguchi M, et al. (2010) Crystal structures of the substrate-bound forms of red
846 chlorophyll catabolite reductase: implications for site-specific and stereospecific reaction. J Mol Biol
847 402:879–891.

848 Suzuki T, Shioi Y (2002) Re-examination of Mg-dechelation reaction in the degradation of chlorophylls using
849 chlorophyllin *a* as substrate. Photosynth Res 74:217–223.

850 Suzuki Y, Amano T, Shioi Y (2006) Characterization and cloning of the chlorophyll-degrading enzyme
851 pheophorbidase from cotyledons of radish. Plant Physiol 140:716–725.

852 Suzuki Y, Doi M, Shioi Y (2002) Two enzymatic reaction pathways in the formation of pyropheophorbide *a*.
853 Photosynth Res 74:225–233.

854 Suzuki Y, Shioi Y (1999) Detection of chlorophyll breakdown products in the senescent leaves of higher plants.
855 Plant Cell Physiol 40:909–915.

856 Suzuki Y, Tanabe K, Shioi Y (1999) Determination of chemical oxidation products of chlorophyll and porphyrin
857 by high-performance liquid chromatography. J Chromatogr A. 839:85–91.

858 Tanaka R, Hirashima M, Satoh S, Tanaka A (2003) The *Arabidopsis-accelerated cell death* gene *ACD1* is
859 involved in oxygenation of pheophorbide *a*: inhibition of pheophorbide *a* oxygenase activity does not
860 lead to the "stay-green" phenotype in *Arabidopsis*. Plant Cell Physiol 44:1266–1274.

861 Tanaka R, Tanaka A (2011) Chlorophyll cycle regulates the construction and destruction of the light-harvesting
862 complexes. Biochim Biophys Acta 1807:968–976.

863 Tang Y, Li M, Chen Y, et al. (2011) Knockdown of OsPAO and OsRCCR1 cause different plant death
864 phenotypes in rice. J Plant Physiol 168:1952–1959.

865 Thomas H, Howarth CJ (2000) Five ways to stay green. J Exp Bot 51:329–337.

866 Tommasini R, Vogt E, Fromenteau M, et al. (1998) An ABC transporter of *Arabidopsis thaliana* has both
867 glutathione-conjugate and chlorophyll catabolite transport activity. Plant J 13:773–780.

868 Tsuchiya T, Ohta H, Okawa K, et al. (1999) Cloning of chlorophyllase, the key enzyme in chlorophyll
869 degradation: finding of a lipase motif and the induction by methyl jasmonate. Proc Natl Acad Sci U S A
870 96:15362–15367.

871 Valentin HE, Lincoln K, Moshiri F, et al. (2006) The *Arabidopsis vitamin E pathway gene5-1* mutant reveals a
872 critical role for phytol kinase in seed tocopherol biosynthesis. Plant Cell 18:212–224.

873 Vergeiner C, Banala S, Kräutler B (2013) Chlorophyll breakdown in senescent banana leaves: catabolism
874 reprogrammed for biosynthesis of persistent blue fluorescent tetrapyrroles. Chem Eur J. doi:
875 10.1002/chem.201301907

876 Vicentini F, Iten F, Matile P (1995) Development of an assay for Mg-dechelatase of oilseed rape cotyledons,
877 using chlorophyllin as the substrate. Physiol Plant 94:57–63.

878 Wagner D, Przybyla D, op den Camp R, et al. (2004) The genetic basis of singlet oxygen-induced stress
879 responses of *Arabidopsis thaliana*. Science 306:1183–1185.

880 Willstätter R, Stoll A (1911) Examinations on chloropyll, XI Chlorophyllase. Justus Liebigs Ann Chem 378:18–
881 72.

882 Wüthrich KL, Bovet L, Hunziker PE, et al. (2000) Molecular cloning, functional expression and characterisation
883 of RCC reductase involved in chlorophyll catabolism. Plant J 21:189–198.

884 Yao N, Greenberg JT (2006) *Arabidopsis* ACCELERATED CELL DEATH2 modulates programmed cell death.
885 Plant Cell 18:397–411.

886 Zhang K, Gan S-S (2012) An abscisic acid-AtNAP transcription factor-SAG113 protein phosphatase 2C
887 regulatory chain for controlling dehydration in senescing *Arabidopsis* leaves. Plant Physiol 158:961–
888 969.

889 Zhou C, Han L, Pislariu C, et al. (2011) From model to crop: functional analysis of a STAY-GREEN gene in the
890 model legume *Medicago truncatula* and effective use of the gene for Alfalfa improvement. Plant
891 Physiol 157:1483–1496.

892 FIGURE LEGENDS

893

894 Figure 1. Chl breakdown by the PAO pathway. Enzymes and their target sites (dashed circles) are indicated.
895 Magnesium, phytol, formate and methanol, the major by-products of the PAO pathway, are also depicted. Side
896 chain residues (R^1-R^4) of the to date characterized NCCs, DNCCs and FCCs are listed in Table 1. Inset: Chl
897 breakdown leads to the formation of water soluble non-phototoxic catabolites. Relevant pyrrole rings and carbon
898 atoms are labelled in the structure of Chl *a*. For abbreviations, see text.

899

900 Figure 2. Topology of Chl breakdown. Proteins involved in the degradation of phototoxic intermediates in the
901 chloroplast are depicted in red, translocation mechanisms across the chloroplast envelope and the tonoplast in
902 blue and enzymes that modify FCC side chains in brown. See text for more information and abbreviations.

903

904 Figure 3. UV/Vis spectra of FCCs, NCCs, DNCCs and YCCs. The YCC spectrum is adapted from Moser et al.
905 (2008a).

906

907 Figure 4. Schematic representation of the loss of absorption capacity of different Chl catabolites during Chl
908 breakdown. The enzymes having a direct influence on the UV/Vis spectra of the Chl catabolites are shown. The
909 UV/Vis spectra are schematically drawn. Note that relative absorptions cannot be compared between different
910 catabolites.

Table 1. List of FCCs, NCCs and DNCCs identified from higher plants

Name	R[1c]	R[2c]	R[3c]	R[4c]	C1-epimer[d]	Source[e]	Reference
***p*FCCs**							
*p*FCC	H	CH_3	Vinyl	H	1	E	(Mühlecker et al. 1997)
epi-*p*FCC	H	CH_3	Vinyl	H	*epi*	E	(Mühlecker et al. 2000)
***m*FCCs**							
At-FCC-1[a]	OH	H	Vinyl	H	1	L	(Pružinská et al. 2005)
At-FCC-2[a]	H	H	Vinyl	H	1	L	(Pružinská et al. 2005)
***hm*FCCs**							
Mc-FCC-49[b]	*O*-glucosyl	CH_3	Vinyl	Daucic acid	*epi*	F	(Moser et al. 2009)
Mc-FCC-56[b]	OH	CH_3	Vinyl	Daucic acid	*epi*	F	(Moser et al. 2008b)
Ma-FCC-61[b]	OH	CH_3	Vinyl	Digalactosylglyceryl	*epi*	L	(Banala et al. 2010)
Ma-FCC-63/64[b]	OH	CH_3	Vinyl	Glucopyranosyl	*epi*	L	(Vergeiner et al. 2013)
Ma-FCC-69[b]	OH	CH_3	Vinyl	3,4-dihydroxyphenyl-ethyl-glucopyranosyl	*epi*	L	(Vergeiner et al. 2013)
Sw-FCC-62[b]	OH	CH_3	Vinyl	Dihydroxyphenyl-ethylglucosyl	1	L	(Kräutler et al. 2010)
NCCs							
At-NCC-1[a]	*O*-glucosyl	H	Vinyl	H	1	L	(Pružinská et al. 2005)
At-NCC-2[a]	OH	H	Vinyl	H	1	L	(Pružinská et al. 2005)
At-NCC-3[a]	OH[f]	H	Vinyl	H	1	L	(Pružinská et al. 2005)
At-NCC-4[a]	*O*-glucosyl	CH_3	Vinyl	H	1	L	(Pružinská et al. 2005)
At-NCC-5[a]	H	H	Vinyl	H	1	L	(Pružinská et al. 2005)
Bn-NCC-1[a]	*O*-malonyl	H	Vinyl	H	1	L	(Mühlecker and Kräutler 1996)
Bn-NCC-2[a]	*O*-glucosyl	H	Vinyl	H	1	L	(Mühlecker and Kräutler 1996)
Bn-NCC-3[a]	OH	H	Vinyl	H	1	L	(Mühlecker and Kräutler 1996)
Bn-NCC-4[a]	H	H	Vinyl	H	1	L	(Pružinská et al. 2005)
Cj-NCC-1[a]	OH	CH_3	Vinyl	H	*epi*	L	(Curty and Engel 1996)
Cj-NCC-2[a]	H	CH_3	Vinyl	H	*epi*	L	(Oberhuber et al. 2003)
Hv-NCC-1[a]	OH	CH_3	Dihydroxyethyl	H	1	L	(Kräutler et al. 1991)
Lo-NCC-1[a]	OH	CH_3	Vinyl	H	nd	L	(Iturraspe et al. 1995)
Ls-NCC-1[a]	OH	CH_3	Vinyl	H	nd	L	(Iturraspe et al. 1995)
Ms-NCC-2[a]	OH	CH_3	Vinyl	H	*epi*	F	(Müller et al. 2007)
Nr-NCC-1[a]	*O*-glucosylmalonyl	CH_3	Vinyl	H	*epi*	L	(Berghold et al. 2004)
Nr-NCC-2[a]	*O*-glucosyl	CH_3	Vinyl	H	*epi*	L	(Berghold et al. 2004)
Pc-NCC-1[a]	*O*-glucosyl	CH_3	Vinyl	H	*epi*	F	(Müller et al. 2007)
Pc-NCC-2[a]	OH	CH_3	Vinyl	H	*epi*	F	(Müller et al. 2007)
So-NCC-1[a]	OH	H	Dihydroxyethyl	H	*epi*	L	(Berghold et al. 2002)
So-NCC-2[a]	OH	CH_3	Dihydroxyethyl	H	*epi*	L	(Oberhuber et al. 2001)
So-NCC-3[a]	OH	H	Vinyl	H	*epi*	L	(Berghold et al. 2002)
So-NCC-4[a]	OH	CH_3	Vinyl	H	*epi*	L	(Berghold et al. 2002)
So-NCC-5[a]	H	CH_3	Vinyl	H	*epi*	L	(Berghold et al. 2002)
Sw-NCC-58[b]	OH	CH_3	Vinyl	H	1	L	(Kräutler et al. 2010)
Tc-NCC-1	*O*-glucosyl	CH_3	Dihydroxyethyl	H	*epi*	L	(Scherl et al. 2012)
Tc-NCC-2	*O*-glucosyl	CH_3	Vinyl	H	*epi*	L	(Scherl et al. 2012)
Zm-NCC-1[a]	*O*-glucosyl	CH_3	Dihydroxyethyl	H	*epi*	L	(Berghold et al. 2006)
Zm-NCC-2[a]	*O*-glucosyl	CH_3	Vinyl	H	*epi*	L	(Berghold et al. 2006)
DNCCs							
Hv-UCC-1[a,g,h]	OH	CH_3	Dihydroxyethyl	H	1	L	(Losey and Engel 2001)
Ap-UCC-1[a,g,h]	OH	CH_3	Dihydroxyethyl	H	*epi*	L	(Müller et al. 2011)
At-NDCC-1	OH	H	Vinyl	H	*epi*	L	(Christ et al. 2013)
YCCs							
Cj-YCC-1	OH	CH_3	Vinyl	H	*N/A*	L	(Moser et al. 2008a)
Tc-YCC-1	*O*-glucosyl	CH_3	Dihydroxyethyl	H	*N/A*	L	(Scherl et al. 2012)

Adapted from (Hörtensteiner 2012)

[a] A nomenclature for NCCs (and FCCs) has been defined (Ginsburg and Matile 1993) in which a prefix indicates the plant species and a suffix number indicates decreasing polarity in reversed-phase HPLC

[b] These catabolites are indexed according to their retention time in HPLC analysis. *Ap Acer platanoides*, *At Arabidopsis thaliana*, *Bn Brassica napus*, *Cj Cercidiphyllum japonicum*, *Hv Hordeum vulgare*, *Lo Liquidambar orientalis*, *Ls Liquidambar styraciflua*, *Ma Muca acuminate*, *Mc Musa cavendish*, *Ms Malus sylvestris*, *Nr Nicotiana rustica*, *Pc Pyrus communis*, *So Spinacia oleracea*, *Sw Spathiphyllum wallisii*, *Tc Tilia cordata*, *Zm Zea mays*

[c] R^1–R^4 indicate residues at C^3, $C8^2$, $C13^2$ and $C17^3$ side positions, respectively, of FCCs, NCCs, DNCCs and YCCs as shown in Figure 1

[d] C1 stereochemistry refers to the type of *p*FCC, i.e. *p*FCC (1) or *epi*-*p*FCC (*epi*), formed in the respective species or genus; nd, not determined; N/A, not applicable

[e] Source of material used for catabolite isolation: E, in vitro enzymatic PAO/RCCR assays; F, fruits; L, leaves

[f] In *At*-NCC-3, the site of hydroxylation is indicated to be C7 (rather than $C8^2$) (Müller et al. 2006)

[g] *Hv*-UCC-1 and *Ap*-UCC-1 are indicated to be pseudo-enantiomers (Müller et al. 2011)

[h] DNCCs have earlier been named urobilinogenoidic Chl catabolites (UCCs)

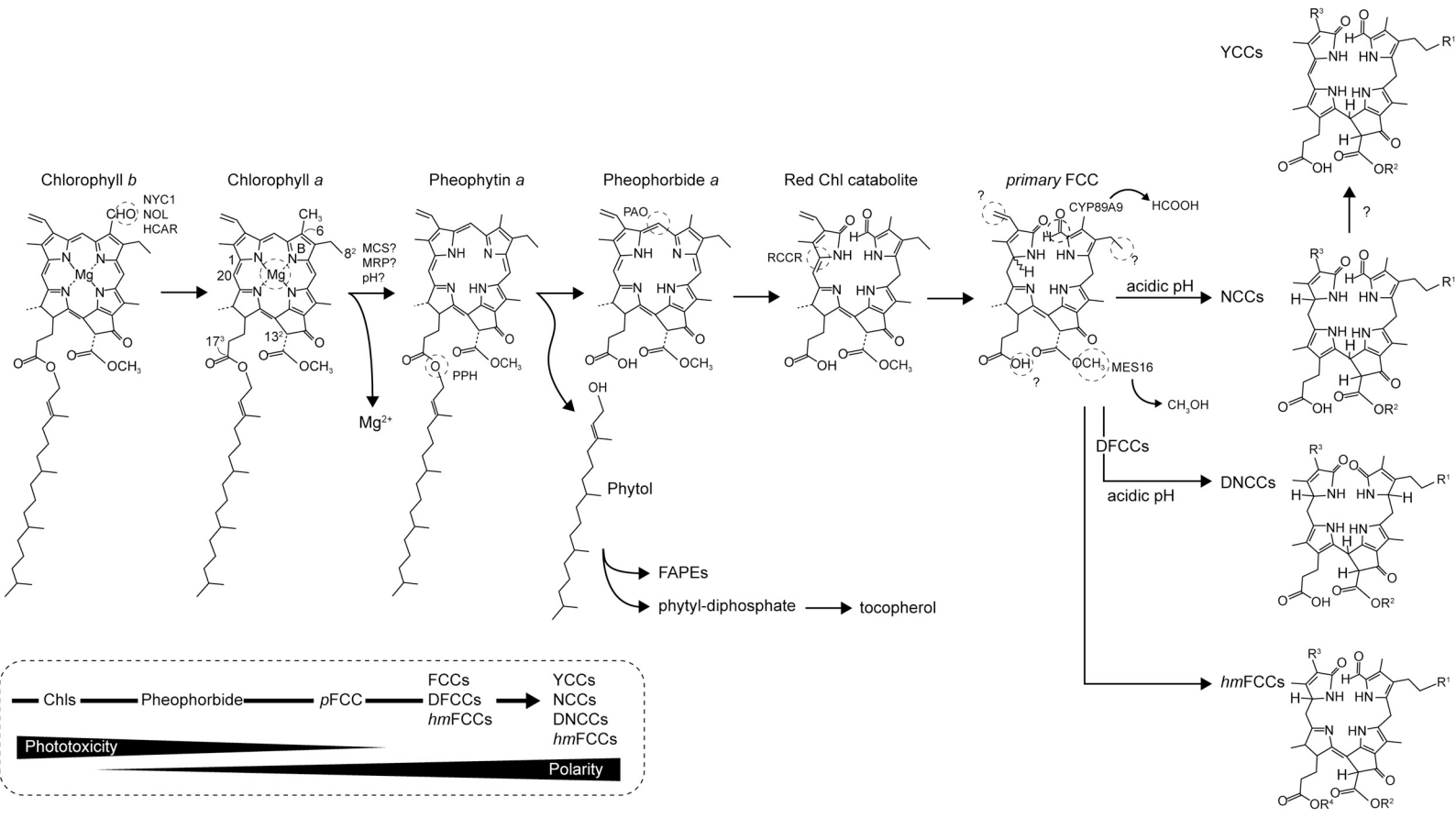
Chlorophyll b
NYC1
NOL
HCAR
Chlorophyll a
MCS?
MRP?
pH?
Mg2+
Pheophytin a
PPH
Pheophorbide a
PAO
Red Chl catabolite
RCCR
primary FCC
CYP89A9
HCOOH
acidic pH
NCCs
YCCs
MES16
CH3OH
DFCCs
acidic pH
DNCCs
hmFCCs
Phytol
FAPEs
phytyl-diphosphate
tocopherol
Chls
Pheophorbide
pFCC
FCCs
DFCCs
hmFCCs
YCCs
NCCs
DNCCs
hmFCCs
Phototoxicity
Polarity

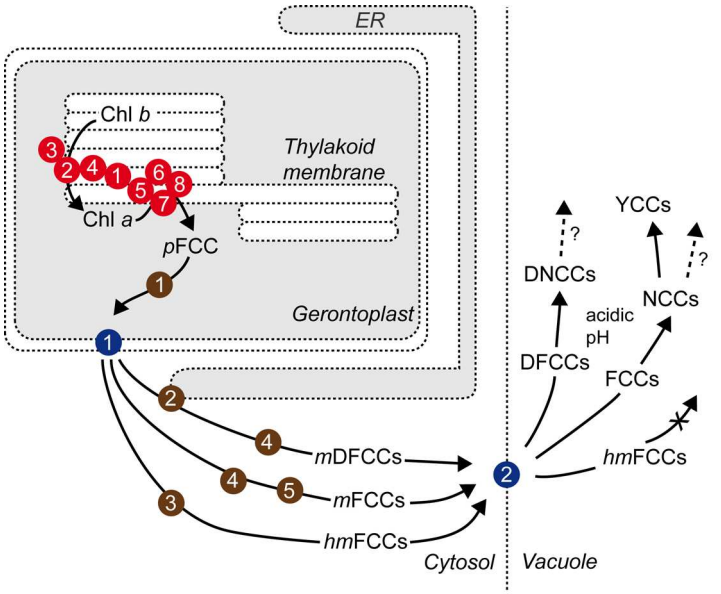

DEGRADATION OF PHOTOTOXIC CATABOLITES

1. SGR
2. NYC1
3. NOL
4. HCAR
5. MCS or MRP?
6. PPH
7. PAO
8. RCCR

TRANSPORT

1. ABC transporters?
2. ABC transporters

MODIFICATIONS OF COLORLESS CATABOLITES

1. ? C8^{2}-*hydroxylation*
2. CYP89A9
3. ? C17^{3}-*hypermodifications*
4. MES16
5. ? *glucosylation / malonylation*

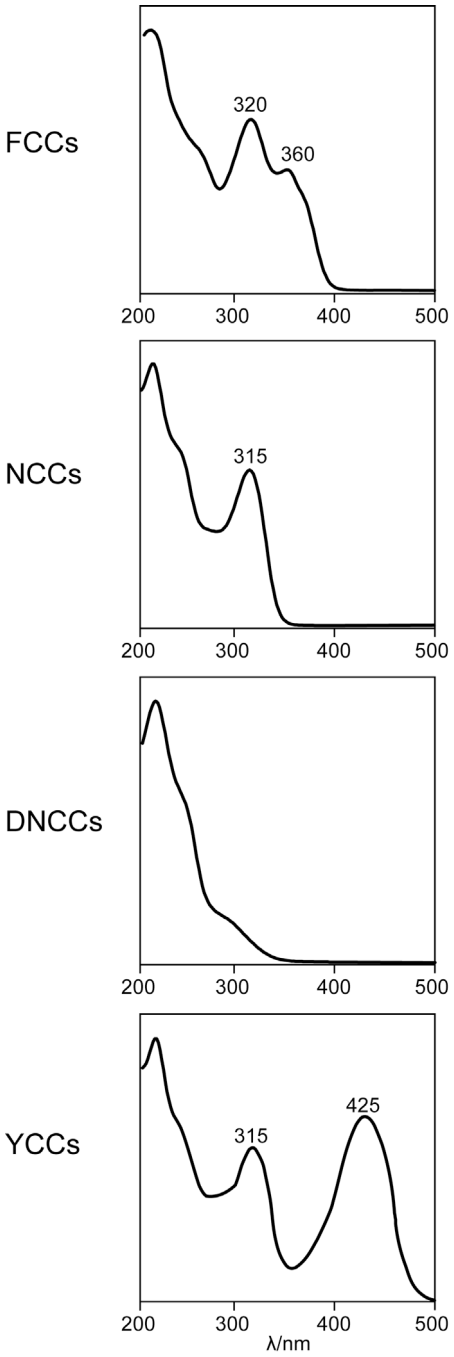
FCCs
320
360
200
300
400
500
NCCs
315
200
300
400
500
DNCCs
200
300
400
500
YCCs
315
425
200
300
400
500
λ/nm

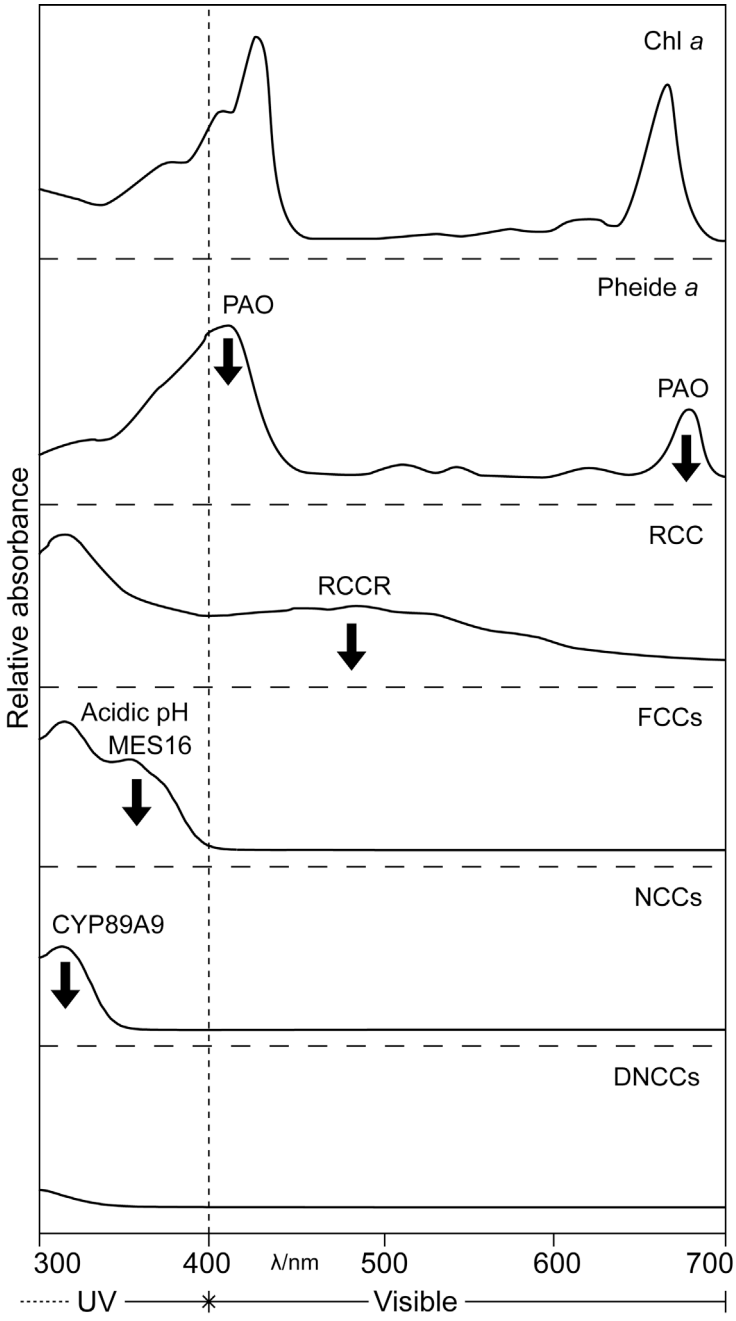
Chl a
Pheide a
PAO
PAO
RCC
RCCR
FCCs
Acidic pH
MES16
NCCs
CYP89A9
DNCCs
Relative absorbance
300
400
λ/nm
500
600
700
UV
Visible